Development of Electrochemical Techniques for Defect Engineering on Advanced Energy Materials

NAKAMURA Takashi

Highly efficient energy storage/conversion devices such as fuel cells and advanced batteries are expected as key technologies for carbon-neutral and sustainable society by utilizing clean hydrogen. In energy functional materials for above-mentioned applications, defects like oxygen vacancy play an important role for their material functionalities. Therefore, understanding true properties of defect is essentially important for defect engineering. The author has been working on the establishment of electrochemical techniques which enable direct evaluation on defect functionality. Furthermore, we have been developing defect control technologies. In this paper, some examples of defect engineering on catalysts and battery materials are given.

Introduction

For the realization of carbon-neutral and sustainable society, efficient utilization of renewable energy is essential. For that, advancing energy conversion/storage technologies such as hydrogen production, rechargeable batteries, electrolysis and fuel cells are important. Cation doping is the most common and effective strategy to advance functionalities of the component of above-mentioned energy conversion/storage devices. However, cation doping is becoming less effective since it has been widely examined so far. For further development of energy functional materials, we focus on the utilization of defects which inherently exist in the materials and play an important role for catalytic, electric and electrochemical properties. It is important to understand decisive factors for the functionalities and establish rational guidelines for defect engineering based on fundamental sciences. Moreover, developing defect control technology is also important goal of our work to exceed the present limit of the material exploration. For the first topic, we have been working on the development of functional energy materials which inherently contain electrochemically active point defects such as oxygen vacancy (unoccupied oxygen site) and interstitial oxygen (excess oxygen at cryptographically vacant space), and for the second topic, we advanced the electrochemical cell as a reactor which can flexibly control defect structure in the target material. Impacts and future benefit of the applicant's work is summarized in Figure 1.

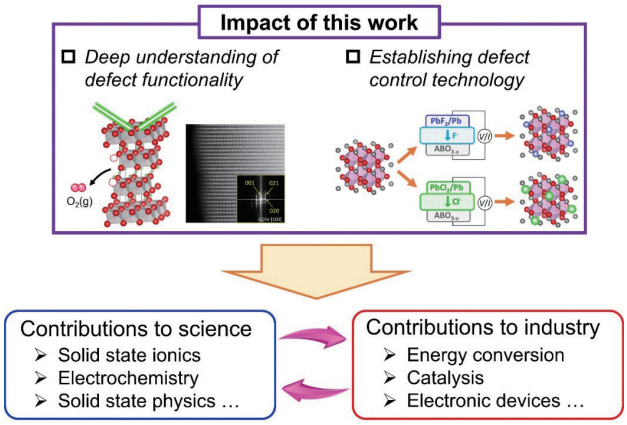

Figure 1 Impacts and future benefits of the present work.

Formation of oxygen defects in layered perovskite oxides $(La,Sr)_2NiO_{4+\delta}$

Perovskite-related oxides are regarded as promising water splitting catalysts and electrode materials for fuel cells.[1-3] Their catalytic properties are strongly influenced by oxygen defects such as oxygen vacancy and interstitial oxygen, and therefore, understanding the mechanism of oxygen defect formation is essentially important. Here, to investigate oxygen defect formation in layered perovskite oxides $(La,Sr)_2NiO_{4+\delta}$ (Figure 2-a), we applied two experimental techniques. One was the thermogravimetry (TG) which can evaluate oxygen content variation by detecting the weight change due to oxygen defect formation, Δw_s, and the other was coulometric titration (CT) which can evaluate oxygen content and equilibrium oxygen chemical potential by using the electrochemical cell composed of an oxide-ion conductor. For TG, very accurate symmetrical balance is installed into glass/ceramics chamber where temperature and atmospheric condition are controlled by a heater and gas-mixtures (Figure 2-b). Variation of oxygen content can be evaluated from the weight change by

$$\Delta\delta = \frac{M_s}{M_O}\frac{\Delta w_s}{w_s} \qquad (1)$$

where $\Delta\delta$, M_s, M_O, and w_s are the relative variation of oxygen nonstoichiometry, the formula weight of the sample and oxygen atom, and the weight of the specimen, respectively. Controllable $P(O_2)$ range by O_2-Ar gas-mixtures is 10^{-4} to 1 bar. This is not enough to evaluate the oxygen defect formation in $(La,Sr)_2NiO_{4+\delta}$.

During the CT measurement, the amount of oxygen in the specimen was controlled by the electric charge passed through the cell. After a specified amount of electric charge was passed, $\Delta\delta$ was calculated by the equation

$$\Delta\delta = \frac{C}{2FM_s} \qquad (2)$$

where C and F is the total amount of electric charge and the Faraday constant, respectively. Equilibrium oxygen partial pressure, $P(O_2)_{eq}$, corresponding to a certain oxygen content was obtained from the electromotive force between the inside and the outside of the cell, E, under the equilibrium state as

$$P(O_2)_{eq} = P(O_2)_{RE}\exp\left(\frac{4FE}{RT}\right) \qquad (3)$$

where $P(O_2)_{RE}$, R, and T are the oxygen partial pressure at the reference electrode, the gas constant and the temperature, respectively. The oxygen content was determined by the weight change of the sample after reduction decomposition under hydrogen atmosphere.

Figure 2-b, 2-c and 2-d shows the oxygen content variation of $La_2NiO_{4+\delta}$, $La_{1.8}Sr_{0.2}NiO_{4+\delta}$ and $La_{1.6}Sr_{0.4}NiO_{4+\delta}$ as a function of equilibrium oxygen partial pressure.[4] Since both TG and CT were applied complementary in this work, oxygen defect formation under wide $P(O_2)$ range was successfully evaluated. $La_{1.8}Sr_{0.2}NiO_{4+\delta}$ showed representative oxygen content variation behavior of a layered perovskite oxide. In high $P(O_2)$ atmosphere, $La_{1.8}Sr_{0.2}NiO_{4+\delta}$ showed oxygen-excess composition by accepting interstitial oxygen in the rock-salt structure, while it showed oxygen-deficient composition by oxygen vacancy formation in low $P(O_2)$ atmosphere. Plateau-like behavior of the oxygen content against $P(O_2)$ was reasonably observed near the stoichiometric oxygen composition ($4+\delta \sim 4.00$) which is consistent with thermodynamic estimation.[5] Such oxygen defect formation also depends on the acceptor concentration, Sr content in this system. As Sr concentration increases, the oxygen vacancy formation proceeds easier, while the formation of interstitial oxygen needs stronger driving force.

The observed oxygen defect formation mechanism was investigated by defect chemical and thermodynamic analyses. The defect equilibrium model was established from the site conservation, defect equilibrium reactions and charge neutrality under the rigid band approximation with p-type degenerated electronic state

$$P(O_2)^{1/2} = \frac{[O_i'']}{[V_i^{\times}]} \exp\left[\frac{\Delta G_I^{\circ} - a[O_i'']}{RT} + 2\ln\left\{\exp\left(\frac{N_A}{D_{VB}V_m}[h^{\bullet}]\right) - 1\right\}\right] \quad (4\text{-}1)$$

$$[O_i''] = \frac{-(6K_f - \delta + K_f\delta) + \sqrt{(6K_f - \delta + K_f\delta)^2 + 8K_f(1 - K_f)(4 + \delta)}}{2(1 - K_f)} \quad (4\text{-}2)$$

where $[O_i'']$, $[V_i^{\times}]$, $[h^{\bullet}]$, ΔG_I°, ΔG_f°, K_f, a, and D_{VB} are the molar concentration of interstitial oxygen, that of vacant interstitial site, that of hole, the Gibbs free energy change of interstitial oxygen formation, that of oxygen Frenkel formation, the equilibrium constant of oxygen Frenkel defect formation, the regular solution parameter and the density of state of the valence band. The derivation of the above defect equilibrium model is summarized in our work.[4] The calculated δ-T-$P(O_2)$ relation is added in Figures 2-b, 2-c and 2-d. As illustrated, the defect equilibrium model can explain oxygen composition variation with T and $P(O_2)$ very well, meaning that the defect structure under certain T and $P(O_2)$ can be estimated precisely by this model. Such fundamental knowledge about oxygen defect formation is essentially important to design defect structures and maximize the functionalities of oxygen defects.

Lattice oxygen stability in lithium-ion battery cathode materials Li(Ni,Co,Mn)O_2

Transition metal oxides are key components of secondary batteries such as alkali metal-ion and anion batteries, sufficient stability of which is thus vitally important for ensuring high energy density and safety. However, problems attributed to the lattice oxygen instability in transition metal oxide cathodes have been widely reported, such as capacity degradation, gas generation and catastrophic thermal runaway.[6,7] These highlights the importance of insight into decisive factors for lattice oxygen stability. In this section, our recent works on the evaluation of lattice oxygen stability in layered rock-salt Li(Ni,Co,Mn)O_2 are summarized. We succeeded to evaluate the oxygen release behavior

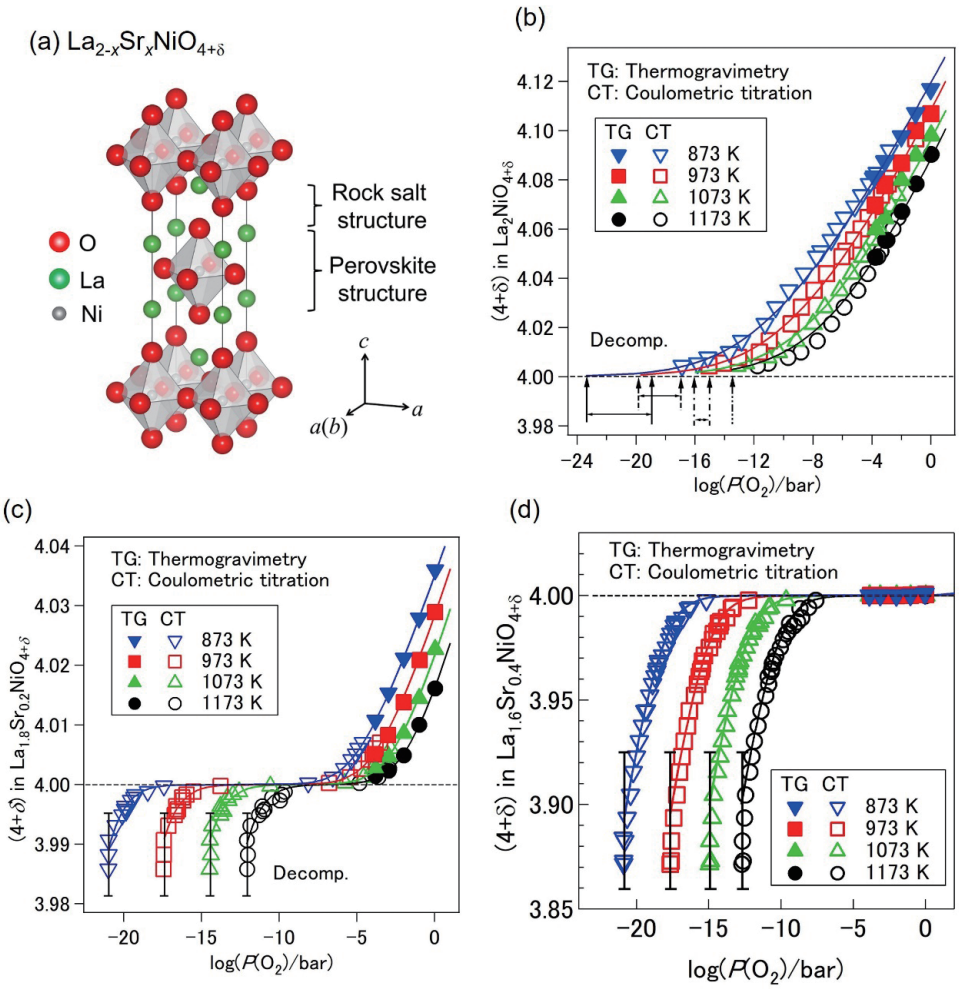

Figure 2 (a) Crystal structure of $(La,Sr)_2NiO_{4+\delta}$. Oxygen content variation (oxygen nonstoichiometry) of (b) $La_2NiO_{4+\delta}$, (c) $La_{1.8}Sr_{0.2}NiO_{4+\delta}$ and (d) $La_{1.6}Sr_{0.4}NiO_{4+\delta}$ as a function of equilibrium oxygen partial pressure. Closed and open symbols were measured by thermogravimetry and by coulometric titration, respectively. Calculated δ-T-$P(O_2)$ relation by the defect equilibrium model (Eq. 4) are shown as solid lines.

of lithium-ion battery cathode by applying the high-temperature solid-state-ionic techniques shown in the previous section, namely TG and CT. Oxygen release behavior and relevant changes in crystal and electronic structures were investigated and analyzed based on defect chemistry and thermodynamics.[8,9]

The molar ratio of oxygen over transition metal, O/TM, against $P(O_2)$ in $LiNi_{1/3}Co_{1/3}Mn_{1/3}O_2$ (NCM111) is summarized in Figure 3-a. In the figure, O/TM = 2 represents the stoichiometric oxygen composition and O/TM < 2 represents the oxygen deficient composition. The oxygen content of the pristine NCM111 was determined by iodometric titration. The oxygen content decreased along with lower equilibrium $P(O_2)$ in the gaseous phase. With totally 4.8 mol% oxygen deficiency introduced in the lattice, NCM111 remained its original layered rock-salt structure without phase transformation or reduction decomposition as confirmed by XRD (Figure 3-b). All XRD profiles of the oxygen-deficient NCM111 were indexed by $R\bar{3}m$, and no impurity peak was observed by oxygen release. However, gradual broadening of diffraction peaks was observed with increasing oxygen deficiency. This indicated the deterioration of crystallinity with oxygen deficiency, despite changes of grain size and morphology was not significant. Diffraction peaks shifted to lower angle with oxygen release, indicating the expansion of the crystal lattice. In addition, the intensity ratio the 003 and 004, I_{003}/I_{104}, declined from 1.36 in the pristine to 0.80 in the 4.8 mol% oxygen-deficient NCM111, indicating disorder of the layered structure by anti-site defect formation (exchange of Li and Ni) as reported in earlier works.[10,11] To investigate the charge compensation mechanism due to oxygen release, oxygen-deficient NCM111 (0.5 mol%, 2.0 mol%, 3.5 mol% and 4.8 mol%) were characterized by X-ray absorption spectroscopy (XAS), and transition metal L-edge spectra are summarized in Figure 3-c, 3-d and 3-e. Probing depth of the fluorescence X-ray mode is typically hundreds nanometers which is close to the size of as-synthesized primary particles, therefore obtained data reflect the bulk information. In Ni L-edge spectra, the intensity of the peak around 855 eV (L_{III} edge) decreases slightly from the pristine to the samples with 0.5 mol% and 2.0 mol% oxygen deficiency, and keep invariant with further oxygen release. These spectral changes suggest that high-valent Ni was reduced to Ni^{2+} until 2.0 mol% oxygen release, and was invariant by further oxygen release. The reduction behavior observed for Ni suggests the existence of small quantity of Ni^{3+} in the pristine sample, which can be explained by negative defects such as cation vacancy or excess Li at the transition metal site (Li_{TM}''). In Co L-edge spectra, there was no observable spectral variation until 0.5 mol% oxygen deficiency, while the shoulder peaks around 778 eV in L_{III} edge appeared with 2.0 mol% oxygen release, indicating that Co was reduced from ca. 0.5 mol% of oxygen loss. The increase of shoulder peaks with oxygen loss suggest that Co acted as the main reduction species when the amount of oxygen loss exceeded 0.5 mol%. The absorption spectra of Mn showed no significant change from the pristine to 4.8 mol% oxygen release, meaning that the contribution of Mn^{4+} reduction is negligibly small in NCM111. From the spectral changes at Ni, Co and Mn L-edge, the charge compensation mechanism due to oxygen release in NCM111 can be explained as follows. In the initial stage of oxygen release only high-valent Ni is selectively reduced followed by the selective reduction of Co^{3+} species, while the reduction of Mn^{4+} is negligible.

As discussed, the charge neutrality was balanced by selective reduction of high-valent Ni in the initial stage of oxygen release in NCM111. This strongly indicates that the presence of high-valence Ni significantly destabilizes lattice oxygen and facilitates oxygen release. To confirm this hypothesis, oxygen release from high Ni concentration NCM series, $LiNi_{0.5}Co_{0.2}Mn_{0.3}O_2$ (NCM 523) and $LiNi_{0.6}Co_{0.2}Mn_{0.2}O_2$ (NCM622), were investigated in a similar manner. Because nominal oxidation state of Ni in NCM111, NCM523 and NCM622 is 2, 2.4 and 2.667, respectively, oxygen release easily proceeds in high Ni NCM. As summarized in Figure 3-f, the δ vs. $P(O_2)$ curve of NCM622 appears in higher $P(O_2)$ region than that of NCM111, while NCM523 shows similar oxygen release behavior to NCM622 except 2-δ < 1.93. These results indicate that lattice oxygen is less stable with increasing Ni valence state and support our hypothesis that high-valent Ni destabilizes lattice oxygen. For more quantitative discussion, partial molar enthalpy of oxygen, $(h_O\text{-}h_O^0)$, was calculated from δ-T-$P(O_2)$ relation which represents necessary energy for oxygen release. Figure 3-g shows $-(h_O\text{-}h_O^0)$ as functions of the amount of released oxygen δ and reduction species during oxygen release; circular symbols show Ni reduction and square symbols show Co reduction. As can be clearly confirmed, $-(h_O\text{-}h_O^0)$, in other words necessary energy for oxygen release, essentially depends on reduction transition metal. Oxygen release with Ni reduction needs less than 0.5 eV, while that with Co reduction needs more than 2.0 eV. It can be concluded that the presence of high valent Ni significantly degrades lattice oxygen stability. As demonstrated in this work, thermodynamic evaluation can pave the way for quantitative and direct discussion on lattice oxygen stability of battery materials. Undoubtedly, transition metal oxides play an important role in the next-generation batteries, including not only

advanced lithium-ion batteries but also multivalent metal-ion batteries and alkali metal-ion batteries. Oxygen release and issues induced by lattice oxygen activity are inevitable problems. We expect the methodology demonstrated in this work will establish guidelines of designing and tailoring advanced energy materials for robust and high-energy-density batteries.

Development of electrochemical reactors for anion defect engineering

Since conventional cation doping strategy is becoming less effective due to wide variety of attempts so far, anion doping gains attention as a new strategy for further advancement of energy functional materials. For efficient utilization of functionalities of anion defects, electrochemical reactors for the control of anion defect species have been developing by the authors' research team. The schematic picture of the reactor and superiorities are summarized in Figure 4. The reactor has some great advantages compared with conventional synthesis techniques such as high-pressure synthesis, mechanical milling, topochemical reaction.[12-14] First, the driving force of the anion defect doping can be controlled by the external voltage according to the Nernst equation. When A^{n-} is controlled by the electrochemical reactor, the chemical potential of the neutral A at the target material μ_A is expressed by the Nernst equation by

$$\mu_A = \mu_{A,CE} + nFE \quad (5)$$

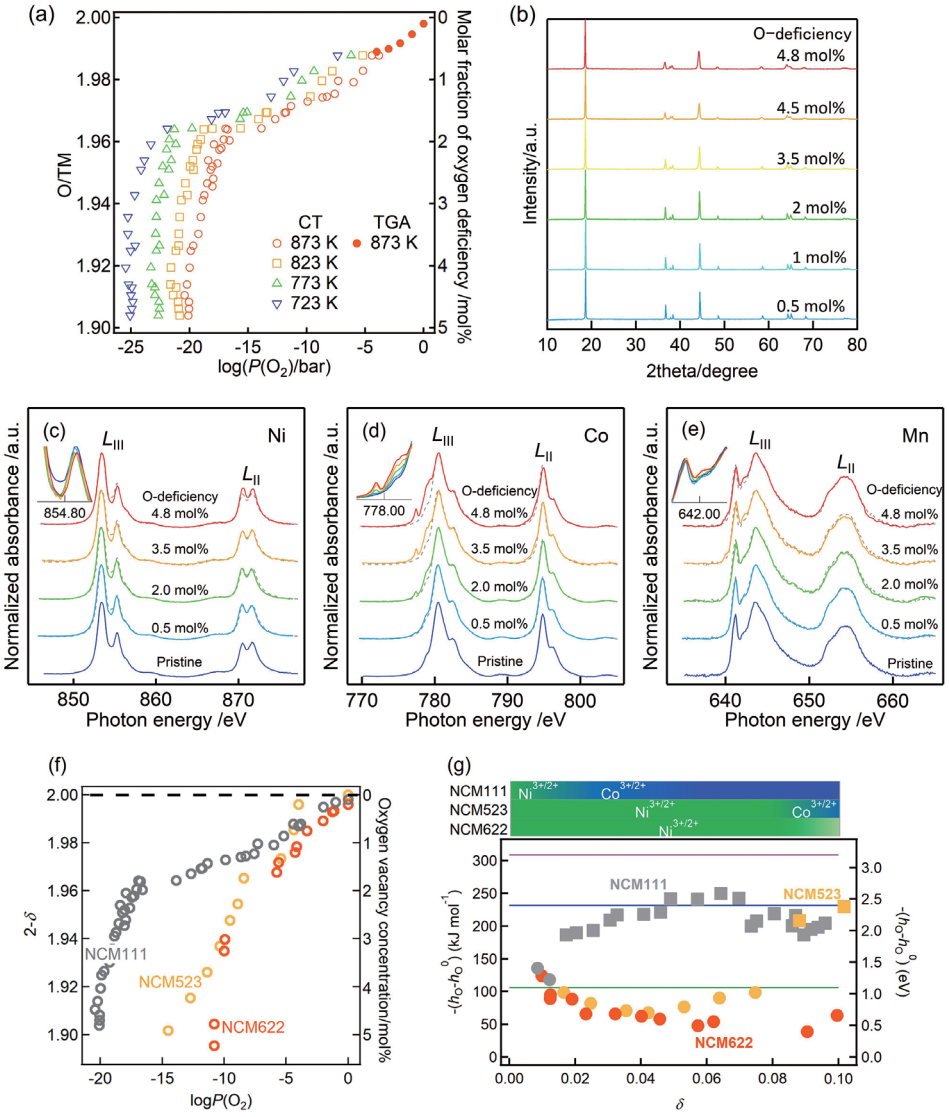

Figure 3 (a) Oxygen release behavior of NCM111 and (b) XRD patterns of oxygen-deficient NCM111. XAS spectra of oxygen-deficient NCM111 at (c) Ni L-, (d) Co L- and (e) Mn L-edge. Oxygen release behavior of NCM111, NCM532 and NCM622 measured at 873 K. (f) $-(h_O-h_O^0)$ as a function of δ. Circular symbols show $-(h_O-h_O^0)$ by Ni reduction and square symbols show that by Co reduction.

where E and $\mu_{A,CE}$ are the electrode potential and the chemical potential of A at the counter electrode, respectively. This means that the reactor can create extremely high activity condition (even impossible condition by conventional techniques) just by applying external voltage. Second, wide variety of anionic defects are controllable by changing the electrolyte. Third, the amount of doped anionic species can be quantitatively controlled by the charge passing through the cell. Considering these advantages, our electrochemical reactor can pave the way to extend the possibility of defect engineering and mixed-anion compounds.

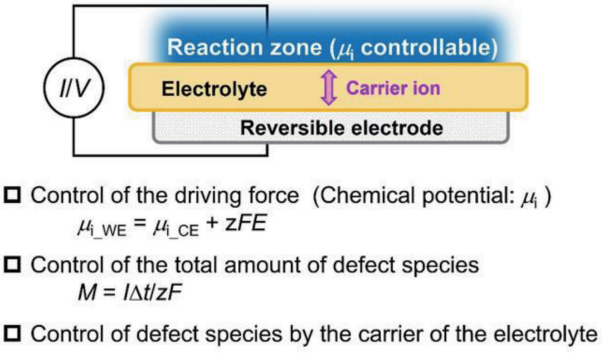

Figure 4 Schematic illustration of the electrochemical reactor for anion defect control.

Conclusions

As a new strategy for further development of energy conversion/storage technologies, we take notice of the utilization of defects in energy functional materials. To achieve this, it is necessary to establish basic sciences regarding defect formation and their functionalities, and to develop a new technology for flexible and easy control of defect species in the target material. As a case study of the first purpose, oxygen defect formation in a layered perovskite oxide $(La,Sr)_2NiO_{4+\delta}$ is summarized, since oxygen defects such as oxygen vacancy and interstitial oxygen play an important role for catalytic activity and electrochemical properties in this material. Oxygen defect formation behavior was investigated, and a defect equilibrium model based on defect chemistry and thermodynamics was proposed. The proposed model agrees very well with observed oxygen content variation with T and $P(O_2)$. Moreover, these experimental and analytical techniques are applied to understand the mechanism of oxygen release from lithium-ion battery cathodes. Although this is an unprecedented challenge in a battery research field, we, for the first time, report fruitful fundamental knowledge of oxygen release. For instance, our work revealed that reduction species (transition metal being reduced during oxygen release) essentially determine the lattice oxygen stability. For the second purpose, we are developing electrochemical reactors composed of an anion conductor which can flexibly, easily and quantitatively control anion defect species in the target material. While the concept of the reactor and schematic illustrations are shown in this paper, some promising results will be shown soon. Complementary advancement of both the establishment of fundamental sciences on defects and the development of defect control techniques is going to contribute to technological innovation of energy functional materials based on defect engineering, and consequently, contribute to the realization of carbon-neutral and sustainable society.

References

[1] A. P. Tarutin, J. G. Lyagaeva, D. A. Medvedev, L. Bi, A. A. Yaremchenko, *J. Mater. Chem. A*, 2021, 9, 154-195.
[2] P. C. Meenu, P. K. Smanta, T. Yoshida, N. J. English, S. P. Datta, S. A. Singh, S. Dinda, C. Chakraborty, S. Roy, *ACS Appl. Energy Mater.*, 2022, 5, 503-515.
[3] H. Li, Y. Chen, J. Ge, X. Liu, A. C. Fisher, M. P. Sherburne, J. W. Ager, Z. J. Xu, *JACS Au*, 2021, 1, 108-115.
[4] T. Nakamura, K. Yashiro, K. Sato, J. Mizusaki, *Solid State Ionics*, 2009, 180, 368-376.
[5] C. Wagner, *Prog. Solid State Chem.* 1971, 6, 1-15.
[6] X. Feng, M. Ouyang, X. Liu, L. Lu, Y. Xia, X. He, *Energy Storage Mater.*, 2018, 10, 246-267.
[7] S. Shrifi-Asl, J. Lu, K. Amine, R. Shahbazian-Yassar, *Adv. Ener. Mater.*, 2019, 9, 1900551.
[8] X. Hou, Y. Kimura, Y. Tamenori, K. Nitta, H. Yamagishi, K. Amezawa, T. Nakamura, *ACS Energy Lett.*, 2022, 7, 1687-1693.
[9] X. Hou, K. Ohta, Y. Kimura, Y. Tamenori, K. Tsuruta, K. Amezawa, T. Nakamura, *Adv. Energy Mater.*, 2021, 11, 2101005.
[10] T. Ohzuku, A. Ueda, M. Nagayama, *J. Electrochem.* Soc., 1993, 140, 1862-1870.
[11] J. Zheng, P. Xu, M. Gu, J. Xiao, N. D. Browning, P. Yan, C. Wang, J. G. Zhang, *Chem. Mater.*, 2015, 27, 1381-1390.
[12] N. Takeda, I. Ikeuchi, R. Natsui, K. Nakura, N. Yabuuchi, *ACS Appl. Energy Mater.*, 2019, 2, 1629-1633.
[13] M. Yang, J. A. Rodgers, L. C. Middler, J. Oró-Sró, A. B. Jorge, A. Fuertes, J. P. Attfield, *Inorg. Chem.*, 2009, 48, 11498-11500.
[14] H. Kageyama, K. Hayashi, K. Maeda, J. P. Attfield, Z. Hiroi, J. M. Rondinelli, K. R. Poeppelmeier, *Nat. Commun.*, 2019, 9, 772.

Dr. NAKAMURA Takashi
Associate Professor,
Institute of Multidisciplinary Research for Advanced Materials,
Tohoku University